STATUS OF THE BNL MUON $(g-2)$ EXPERIMENT[1]

R. Prigl[b] ,H.N. Brown[b], G. Bunce[b], R.M. Carey[a], P. Cushman[h], G.T. Danby[b], P.T. Debevec[g], H. Deng[l], W. Deninger[g], S.K. Dhawan[l], V.P. Druzhinin[i], L. Duong[h], W. Earle[a], E. Efstathiadis[a], F.J.M. Farley[l], G.V. Fedotovich[i], S. Giron[h], F. Gray[g], M. Grosse Perdekamp[l], A. Grossmann[e], U. Haeberlen[f], M. Hare[a], E.S. Hazen[a], D.W. Hertzog[g], V.W. Hughes[l], M. Iwasaki[k], K. Jungmann[e], D. Kawall[l], M. Kawamura[k], B.I. Khazin[i], J. Kindem[h], F. Krienen[a], I. Kronkvist[h], R. Larsen[b], Y.Y. Lee[b], W. Liu[l], I. Logashenko[i], R. McNabb[h], W. Meng[b], J.-L. Mi[b], D. Miller[h], J.P. Miller[a], W.M. Morse[b], P. Neumayer[e], C.J.G. Onderwater[g], Y. Orlov[c], C. Pai[b], C. Polly[g], J. Pretz[l], G. zu Putlitz[e], S.I. Redin[l], O. Rind[a], B.L. Roberts[a], N. Ryskulov[i], R. Sanders[b], S. Sedykh[g], Y.K. Semertzidis[b], S. Serednyakov[i], Yu.M. Shatunov[i], E. Solodov[i], M. Sossong[g], A. Steinmetz[l], L.R. Sulak[a], M. Tanaka[b]m C. Timmermans[h], A. Trofimov[a], D. Urner[g], D. Warburton[b], D. Winn[d], A. Yamamoto[j], D. Zimmerman[h].

[a]Department of Physics, Boston University, Boston, MA 02215, USA, [b]Brookhaven National Laboratory, Upton, NY 11973, USA, [c]Newman Laboratory, Cornell University, Ithaca NY 14853, USA, [d]Fairfield University, Fairfield, CT 06430, USA, [e]Physikalisches Institut der Universität Heidelberg, 69120 Heidelberg, Germany, [f]MPI für Med. Forschung, 69120 Heidelberg, Germany, [g]Department of Physics, University of Illinois, Urbana, IL 61820, USA, [h]Department of Physics, University of Minnesota, Minneapolis, MN 55455, USA, [i]Budker Institute of Nuclear Physics, Novosibirsk, Russia, [j]KEK, Japan, [k]Tokyo Institute of Technology, Tokyo, Japan, [l]Department of Physics, Yale University, New Haven, CT 06511, USA.

ABSTRACT

The muon $(g-2)$ experiment at Brookhaven completed a first run in June and July 1997. The main components of the experiment, which include the superconducting inflector, the superferric storage ring, the electrostatic quadrupoles and the lead-scintillating fiber electron calorimeters, have been commissioned satisfactorily. Our first measurement of the ratio R of the spin precession frequency of the positive muon relative to that of a free proton, $R = (3.707\,219 \pm 0.000\,048) \times 10^{-3}$, is in good agreement with the previous CERN measurements for μ^+ and μ^-, and has approximately the same uncertainty as each of these measurements. In spring 1998 a muon kicker was installed and successfully tested in the storage ring magnet and a significant improvement in the knowledge of the muon g-factor is expected from upcoming runs in August 1998 and January 1999.

I. INTRODUCTION

To the current level of the relative standard uncertainty $u_r = 4 \times 10^{-9}$, the anomalous g factor for the electron,

$$a_{\rm e} \equiv \frac{(g-2)_{\rm e}}{2} \tag{1}$$

arises entirely from virtual photons and electron-positron pairs [1]. The agreement between experimental and theoretical values of $a_{\rm e}$, which is limited by the relative standard uncertainty of about 25×10^{-9} with which the fine structure constant α is known, provides one of the most decisive tests of pure quantum electrodynamics [2].

For the muon, the relative contributions to a_μ of heavier particles or new contact interactions are much larger than for the electron because they usually scale as $(m_\mu/m_e)^2 \approx 4 \times 10^4$. In particular, the fractional contribution from diagrams including virtual hadrons is about 60×10^{-6}, and was observed for the first time in the most recent CERN measurement [3] of a_μ with $u_r = 7 \times 10^{-6}$.

The goal of the new BNL muon $g-2$ experiment is to measure a_μ with $u_r = 0.35 \times 10^{-6}$. With this uncertainty, the electroweak fractional contribution [4] of 1.3×10^{-6}, which arises from virtual processes involving the Z and W vector bosons, should be observed, thus offering an important test of electroweak renormalization. In addition, a sensitive and powerful test for contributions beyond the standard model will be provided, especially for μ and W substructure or anomalous couplings, but also for supersymmetry and leptoquarks [4, 5, 6, 7].

II. THE BROOKHAVEN EXPERIMENT

The principle of the measurement is similar to the third CERN experiment [3]. Polarized muons are stored in a uniform dipole magnetic field with electrostatic quadrupoles providing weak vertical focussing. The muon spin precesses relative to the momentum vector with the frequency

$$\vec{\omega}_a = -\frac{e}{m_\mu}\left[a_\mu \vec{B} - \left(a_\mu - \frac{1}{\gamma_\mu^2 - 1}\right)\vec{\beta}\times\vec{E}\right], \tag{2}$$

[1]Work supported in part by the US Dept. of Energy, The U.S. National Science Foundation, the German Bundesminister für Bildung und Forschung, the Russian Ministry of Science, and the US-Japan Agreement in High Energy Physics.

where $\vec{\beta} = \vec{v}/c$, $\gamma = 1/\sqrt{1 - v^2/c^2}$, and assuming that $\frac{E}{c} \ll B$ and $\vec{\beta} \cdot \vec{B} \approx 0$. The dependence of ω_a on the electric field $\vec{E}$ can be eliminated by storing muons with the "magic" γ_μ=29.3, corresponding to a muon momentum $p_\mu = 3.094$ GeV/c. In this ideal case, $a_\mu - 1/(\gamma_\mu^2 - 1) = 0$, and the focussing electric field does not affect the spin precession frequency. a_μ is then extracted from $\omega_a \approx 2\pi \times 230\,\mathrm{kHz}$ through

$$a_\mu = \frac{\omega_a/\omega_\mathrm{p}}{\mu_\mu/\mu_\mathrm{p} - \omega_a/\omega_\mathrm{p}} \tag{3}$$

where $\omega_\mathrm{p} \approx 2\pi \times 62\,\mathrm{MHz}$ is the free proton precession frequency in the same magnetic field seen by the muons. The ratio of muon to proton magnetic moments, μ_μ/μ_p, is currently known with $u_r = 0.15 \times 10^{-6}$ from the hyperfine structure interval in muonium [8], and is expected to be improved by a recent experiment [9].

The source of the stored muons is the Alternating Gradient Synchrotron (AGS) proton beam, which delivers eight bunches with a total of $\approx 40\times 10^{12}$ protons at 24 GeV/c onto a nickel production target every 2.6 s. The individual bunches have a total width of about 100 ns and are spaced apart by 33 ms.

From each bunch about 4×10^7 pions at $\approx$ 3.1 GeV/c are transported from the target along a 116 m beam line. About 50 % of the pions decay along the transport line and a momentum slit followed by a bending magnet near the downstream end selects either pions or forward decay muons for injection into the storage ring. After passing through a hole in the back of the storage ring magnet yoke and a field free region supplied by a superconducting inflector magnet [10], the pion or muon beam enters the toroidal storage region which has a radius of 7.112 m and a 9 cm diameter cross section. In pion injection mode, our mode of operation in 1997, a small fraction of muons from pion decay, $\pi^+ \to \mu^+\nu_\mu$, are launched onto a stable orbit and are stored.

One of the major improvements over the last CERN experiment is the use of direct muon injection. In this mode, a total kick of $\approx$ 11 mrad on the first one or two turns is needed to store the muons born in the pion decay channel. The muon kicker is a pulsed magnet consisting of three sections of pairs of current sheets, each 1.7 m long. The peak current through the plates during a 300 ns wide pulse is about 4200 A, providing a vertical field of 0.0016 T superimposed on the 1.45 T field of the storage ring magnet.

The continuous superferric 'C'-shaped storage ring magnet, Fig. 1, is excited by superconducting coils which carry a current of 5177 A. The yoke consists of twelve 30 degree sections bolted together at the four corners, with azimuthal gaps of less than 1 mm. The pole pieces are 10 degrees long and aligned with the yoke sectors. The azimuthal gap between adjacent pole pieces of about 75 μm is filled with insulating Kapton foils to avoid irregular eddy current effects. The vertical gap between pole and yoke decouples the yoke and pole pieces, which are fabricated from high quality steel, and allows the insertion of iron wedges to compensate for the C-magnet quadrupole. The 10 cm wide wedges are radially adjustable to improve the field homogeneity in azimuth. The four edge shims, 5 cm wide and about 3 mm high, are the main tool for reducing field variations over the beam cross section. A first adjustment of the shims in preparation for the 1997 run resulted in the field distribution shown in Fig. 2 (a). Since then, the 144 shims have been ground individually and the field homogeneity locally as well as integrated over azimuth has improved significantly. Continuous current shims on the poles, which were installed but not operational in 1997, were commissioned in summer 1998 to further reduce the fractional inhomogeneity in the integrated field. A contour plot from a measurement in August 1998 is shown in Fig. 2 (b).

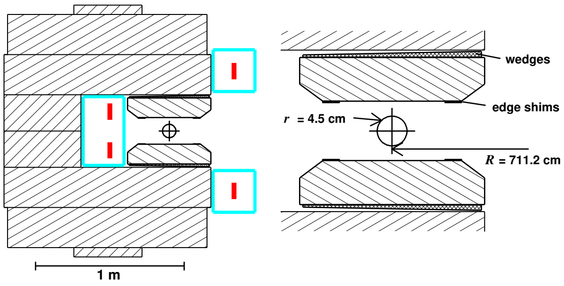

Figure 1: Storage ring magnet cross section and detailed view of the magnet gap region.

The magnetic field is monitored by 366 nuclear magnetic resonance (NMR) probes embedded in the top and bottom plates of the twelve vacuum chambers [11]. The field inside the storage region is mapped several times every week using a trolley containing a matrix of 17 NMR probes which operates in vacuum. The probes in the trolley are calibrated in place against a standard probe [12].

The decay positrons from $\mu^+ \to \mathrm{e}^+\nu_\mathrm{e}\bar{\nu}_\mu$, which constitute our signal, range in energy from 0 GeV to 3.1 GeV, and are detected with 24 Pb-scintillating fiber calorimeters placed symmetrically around the inside of the storage ring. Because of the parity violating nature of the weak decay, the high-energy positrons are preferentially emitted along the muon spin direction. The muon spin precession is reflected in the decay positron spectrum, $N(t)$, where we expect

$$N(t) = N_0 e^{-t/\tau_\mu}\left[1 - A\cos\left(\omega_a t + \phi\right)\right]. \tag{4}$$

The asymmetry parameter, A, is energy dependent. For a positron energy threshold of 1.8 GeV, A is ≈ 0.4.

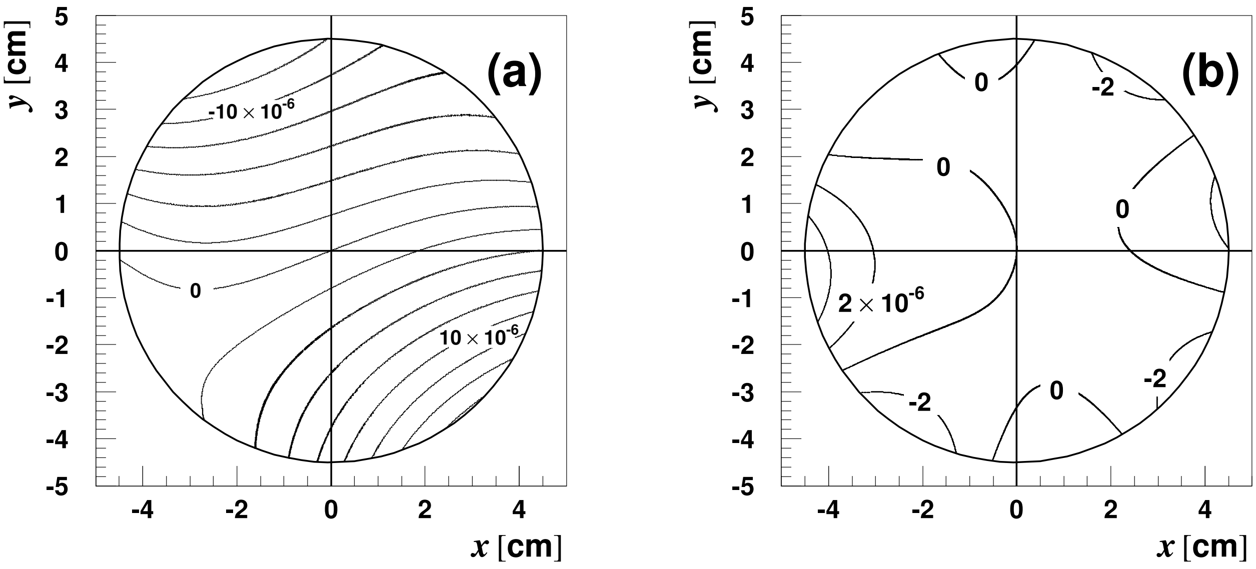

Figure 2: Contour plot of the magnetic field integrated over azimuth during the 1997 run (a) and in August 1998 after additional shimming (b); x denotes the radial and y the vertical direction. Each contour line represents a fractional change of 2×10^{-6}.

The arrival times of the positrons are recorded in multi-hit time-to-digital converters (TDCs), and the calorimeter pulses are also sampled by a custom 400 MHz waveform digitizer (WFD). A laser and light emitting diode (LED) system are used to monitor potential time and gain shifts. Several detector stations are outfitted with a finely segmented hodoscope array of 20×32 small scintillating elements connected to a multianode phototube, which provide position sensitive information on the muon decay positron. Additional event information is derived from five stations each equipped with five scintillator paddles oriented horizontally. Finally, a traceback chamber provides information on the stored muon phase space. The latter has to be convoluted with the magnetic field to determine the average field seen by the muons.

The mean radial distribution of the stored muons can also be obtained from the fast rotation signal from the initial time structure of the injected beam. The results of the analysis were consistent with a uniformly filled phase space. Vertically, the stored beam was approximately 1 mm high due to a nonzero average of the radial field component B_x of about 20×10^{-6} relative to the vertical field.

III. THE RESULT FROM THE 1997 RUN

The exponential muon decay, modulated by the $(g-2)$ precession, from a subset of the data taken in 1997 is shown in Fig. 3. During the offline analysis, a problem associated with an incorrect adjustment of the settings of the custom WFD modules was uncovered. To minimize the data volume, the WFD modules can be set to not sample pulses that exceed the threshold for less than an adjustable minimum time interval, which inadvertently was set too long for the threshold used during data taking. Since the electron pulses ride on a time dependent background arising from the injected pion beam, the average time above threshold was decreasing with increasing time after injection, resulting in a time dependent energy threshold for pulse sampling. Consequently, the asymmetry parameter also changed with time. Thus, the data had to be fit to an 8-parameter function

$$F(t) = N_0 e^{-\frac{t}{\gamma\tau}} \frac{1}{(t-t_0)^\alpha}[1+(A_1 t + A_2)\cos(\omega_a t + \Phi)] + B, \tag{5}$$

where $t_0 = 5\,\mu$s after injection, rather than to the function in Eq. (4). The power law was found to best describe the time dependent background.

The experiment measures the frequency ratio $R = \omega_a/\omega_p$, where ω_p is the proton NMR frequency measured with the beam tube trolley. Including fractional corrections of about 1×10^{-6} from the electric quadrupole field for vertical focusing, we obtain

$$R = 3.707\,220(47)(11) \times 10^{-3} \tag{6}$$

where the first standard uncertainty is statistical and the second systematic. Adding the two uncertainties in quadrature results in $u_r = 13 \times 10^{-6}$. For a_μ we obtain

$$a_\mu = \frac{R}{\lambda - R} = 1\,165\,925(15) \times 10^{-9} \tag{7}$$

where $\lambda = \mu_\mu/\mu_p = 3.183\,345\,47(47)$ [13]. Our result

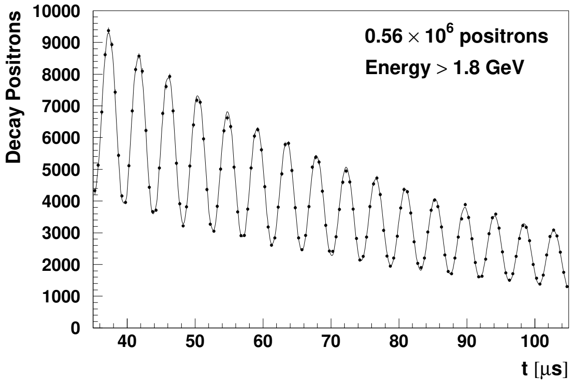

Figure 3: Analysis of decay positron counts as a function of time. The exponential muon decay is modulated at the $(g-2)$ precession period. The solid line represents a fit to the data.

is in good agreement with the last CERN measurement, $a_{\mu,\mathrm{CERN}} = 1\,165\,924(8.5) \times 10^{-9}$ [3] .

Uncertainties associated with systematic effects are listed in Table 1. As even the 8-parameter function fails to describe the signal completely at early times, the fitted frequency depends on the fitting start time and there is an uncertainty associated with the choice of the start time, which in fact is the largest contribution to the uncertainty from systematic effects. This uncertainty as well as the WFD Energy Threshold and Gain and Pedestal Shift contributions are expected to be absent or smaller by at least an order of magnitude in the upcoming runs due to the heavily reduced background in the muon injection mode and the absence of the WFD problem. The only other significant entries in Table 1 are associated with the uncertainty in the knowledge of the average field seen by the muon beam. The improved field homogeneity, the use of active shimming, and the installation of two plunging probes that allow continuous cross calibration of the beam tube trolley, should reduce these uncertainties by about a factor of ten as well.

Table 1: Relative standard uncertainties $u_r/10^{-6}$ from systematic effects

Systematic Effect	$u_r/10^{-6}$
Magnetic field B	1.0
Muon distribution and $< B >$	0.9
WFD energy threshold	1.5
Gain and pedestal shift	0.6
Muon losses	0.2
Timing shifts	0.1
Radial E field, pitch correction	0.05
Fitting start time	2.0
Binning effects	0.2
Total	2.9

IV. OUTLOOK

After successfully commissioning all major components besides the muon kicker in 1997, the muon $(g-2)$ collaboration is preparing for muon injection runs in August 1998 and January 1999. The muon kicker has been operated in the storage ring magnet and will provide a significantly increased muon flux with much lower background levels. Other major improvements include the reduced magnetic field inhomogeneity, substantial increases in the light output of several detector stations for better separation between decay electron pulses and background, and additional beam instrumentation to maximize the number of stored muons per proton on target. The collaboration aims to reduce the uncertainty in R and a_μ by a factor of ten or more relative to the 1997 result in these two runs, and is confident that the proposed relative uncertainty of 0.35×10^{-6} in a_μ can be achieved with additional beamtime.

References

[1] R. van Dyke et al., Phys. Rev. Lett., Vol. 59, No. 1, pp. 26-29, 1987.

[2] T. Kinoshita, Rep. Prog. Phys., Vol. 59, No. 11, pp. 1459-1492, 1996.

[3] J. Bailey et al., Nucl. Phys. B., Vol. B150, No. 1, pp. 1-75, 1979.

[4] T. Kinoshita and W.J. Marciano in Quantum Electrodynamics, ed. T. Kinoshita, Singapore, World Scientific, Ch. 10, pp. 419-478, 1990.

[5] P. Méry et al., Z. Phys. C., Vol. 46, No. 2, pp. 229-252, 1990.

[6] J. Lopez et al., Phys. Rev. D., Vol. 49, No. 1, pp. 366-372, 1994; G. Couture and H. Konig, Phys. Rev. D., Vol. 53, No. 1, pp. 555-557, 1996; U. Chattopadhyay and P. Nath, Phys. Rev. D., Vol. 53, No. 3, pp. 1648-1657, 1996; T. Moroi, Phys. Rev. D., Vol. 53, No. 11, pp. 6565-6575, 1996.

[7] F.M. Renard et al., Phys. Lett. B., Vol. 409, No. 3, pp. 398-404, 1997.

[8] E. R. Cohen and B. N. Taylor, Rev. Mod. Phys., Vol. 59, No. 4, pp. 1121-1148, 1987.

[9] M. G. Boshier et al., Phys. Rev. A., Vol. 52, No. 3, pp. 1948-1953, 1995.

[10] F. Krienen et al., Nucl. Instr. Meth. A., Vol. 283, No. 1, pp. 5-12, 1989.

[11] R. Prigl et al., Nucl. Instr. Meth. A., Vol. 374, No. 1, pp. 118-126, 1996.

[12] X. Fei et al., Nucl. Instr. Meth. A., Vol. 394, No. 3, pp. 349-356, 1997.

[13] Particle Data Group, Phys. Rev. D., Vol. 54, No. 1, pp. 1-720, 1996;